Teaching Nonradiative Transitions with MATLAB and Python

Xin Zheng[1,2], Matthew C. Drummer[1,2], Thomas A. Russell[1], Samer Gozem[3], Ksenija D. Glusac[1,2*]

[1] Department of Chemistry, University of Illinois Chicago, Chicago, Illinois 60607, United States
[2] Chemical Sciences and Engineering Division, Argonne National Laboratory, Lemont, Illinois 60439, United States
[3] Department of Chemistry, Georgia State University, Atlanta, Georgia 30302, United States

*Email: glusac@uic.edu

Abstract

Nonradiative transitions are changes in energy states in atoms, ions or molecules that do not involve the emission or absorption of photons. Despite their importance in understanding luminescent properties and photochemical reaction mechanisms, nonradiative transitions are rarely given more than a qualitative overview in undergraduate and even graduate physical chemistry curricula. To supplement the coverage of nonradiative transition topics, we provide here a set of active learning exercises to help students develop an intuitive understanding of the factors that determine the rate of nonradiative transitions. We start by outlining the theoretical background through the formulation of the Franck-Condon factor and its relation to the rate of nonradiative transition. We then introduce three teaching modules, with associated MATLAB and Python codes, to explore how 1) the excited state nuclear displacement, 2) the electronic energy gap between excited and ground state, and 3) the excited/ground state vibrational mode frequencies affect the magnitude of the Franck-Condon factor and thereby the rate of nonradiative transitions. The wavefunction overlap plots that accompany all teaching modules provide direct visualization of the effect of input parameters on the magnitude of Franck-Condon overlap integral.

Keywords

Upper-Division Undergraduate, Graduate Education / Research, Physical Chemistry, Computer-Based Learning, Hands-On Learning / Manipulatives, Photochemistry, Theoretical Chemistry

Table of Contents Graphic

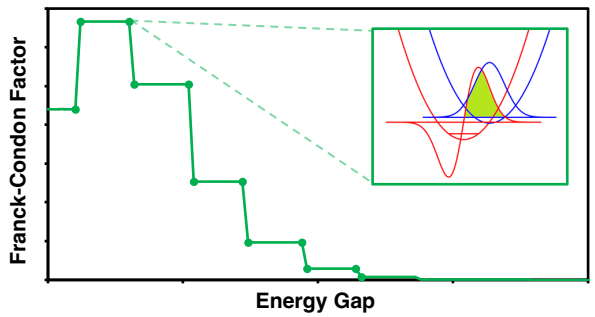

Introduction

Absorption of photons by molecules is accompanied by a large and sudden increase in the molecule's energy (e.g., by 170 – 300 kJ/mol upon absorption of visible light). The molecule typically dissipates this energy through radiative and/or nonradiative transitions.[1] Non-radiative transitions (Non-RTs) are described by two fundamental steps, as illustrated by wavy arrows in the Jablonski state energy diagram of **Scheme 1**. In Jablonski state energy diagrams, the vertical axis represents potential energy at a static geometry. The horizontal lines represent vibrational energy levels for different electronic states, where S_0 is the ground singlet state, S_1 is the first singlet excited state, S_2 is the second singlet excited state, and T_1 is the first triplet state. The lowest vibrational level for each electronic state is bolded. The lines are horizontally displaced to avoid congestion, and the horizontal axis does not represent any physical quantity here. The steps represented by horizontal arrows involve transitions between electronic states of either same or different spin, defining internal conversion (IC) and intersystem crossing (ISC), respectively. Those are shown as green and orange arrows, respectively. The steps represented by vertical red arrows represent the VR of the molecule within the same electronic state. These non-RTs distribute the excitation energy into different vibrational modes of the molecule (intramolecular dissipation) and, in the condensed phase, the vibrational modes of the surrounding bath (intermolecular dissipation), effectively converting the absorbed photon's energy into heat. We focus here on the electronic transitions IC and ISC, processes that typically involve a conversion from the lowest vibrational level of one electronic state (such as S_1 state in **Scheme 1**) to the manifold of vibrationally "hot" states of another electronic state (such as T_1 states in **Scheme 1**).

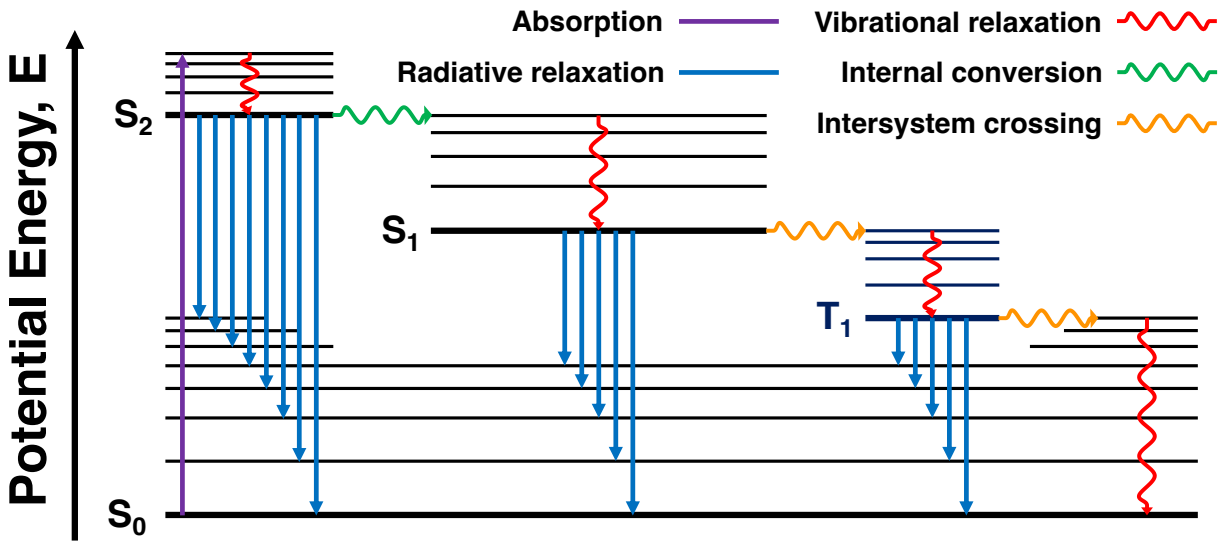

Scheme 1. Jablonski diagram summarizing radiative (absorption, fluorescence and phosphorescence) and nonradiative (vibrational relaxation, internal conversion and intersystem crossing) transitions.

Even though non-RTs are spectroscopically silent, they indirectly influence the spectroscopy and reactivity of emissive molecules. For example, the shape and intensity of emission spectra is dictated by non-RTs, as described by Kasha's rule and energy gap law (EGL).[2-5] The biological chemiluminescence is made possible by the enzyme's ability to suppress non-RT channels. [6-10]

Non-RTs are critical for photochemical transformations taking place in natural vision proteins[11-13] [14-17] and artificial photocatalysts.[18] More details about the role of non-RTs on these processes can be found in Section S1 of the SI. The rates of non-RTs are controlled by, among other parameters, an overlap integral between the vibrational wavefunctions of the initial and final states. The square of this overlap integral is called the Franck-Condon factor (FCF), a concept formulated by James Franck and Edward U. Condon[19-21] to calculate the intensities of absorption bands from vibronic transitions that are concomitant with electronic transitions. To understand non-radiative decay, it is important to move away from the "static nuclei" picture represented by the Jablonski diagram in **Scheme 1** and now consider the variation in the system's potential energy as a function of nuclear motion. Often, this is done in the context of the Born-Oppenheimer approximation, which allows the representation of electronic energy parametrically as a function of changing nuclear coordinates, as shown in **Scheme 2**. Within the framework of the Born-Oppenheimer approximation, the probability of vibronic transitions as jumps between potential energy surfaces can be quantified in terms of FCFs as the overlap between the vibrational wavefunctions of the initial and final electronic states. FCFs, in the context of non-RTs, will be the focus of this technology report. Although the overlap integral itself is occasionally referred to as the FCF,[22] we will keep consistent with the definition given by many contemporary textbooks[2, 23-27] and articles[28-35] and define the overlap integral as the FC overlap and the square of the overlap integral as the FCF. The FCF is a dimensionless parameter that has a value in the range of 0 to 1. The rate of IC is slow for FCF values close to 0 and is fast for FCF values close to 1. The value of the FCF is sensitive to the structural distortion (Δx) and the energy gap (ΔE) between the states involved in the transition, as shown in **Scheme 2**. It is also dependent on the curvatures (vibrational frequencies or wavenumbers, $\tilde{\nu}$) of the potential energy surfaces of the two electronic states.

Despite their importance in molecular spectroscopy and photochemistry, the fundamentals of non-RTs are generally not covered in undergraduate curricula.[36-39] Most undergraduate textbooks describe RTs involving the absorption and emission of light. Please see Section S2 of the Supporting Information for more information about the coverage of non-RTs in textbooks. FCFs are often introduced in the context of RTs because they can be intuitively connected to the line shapes of absorption and emission spectra. Non-RTs do not produce spectroscopic signals that can be correlated to FCFs. Therefore, there is a need to develop alternative visual aids and tools to help students learn about non-RTs. Only in highly specialized textbooks and a few published educational articles do we begin to see an in-depth, physical description of non-RTs.[2, 24-26, 40-44] However, these chemical physics books are not accessible to many chemistry students who do not have the pre-requisite mathematics background to describe the underlining quantum phenomena. Thus, there is a need for teaching tools that can introduce the concepts behind non-RTs to chemistry students.

Here, we provide teaching modules that can be used in undergraduate and graduate physical chemistry classrooms to help students develop intuition for factors that control non-RTs. We provide a set of codes, written in MATLAB and Python, to enable direct visualization of these factors and to complement the theoretical aspects learned in the classroom. MATLAB and Python were selected due to their versatility at illustrating topics in chemical education[45-56] and because they are readily available to students. The Background section of the article provides a brief description of IC and ISC through the framework of perturbation theory. The Modules section provides a description of three teaching modules that illustrate how IC is affected by the parameters that describe molecular potential energy surfaces.

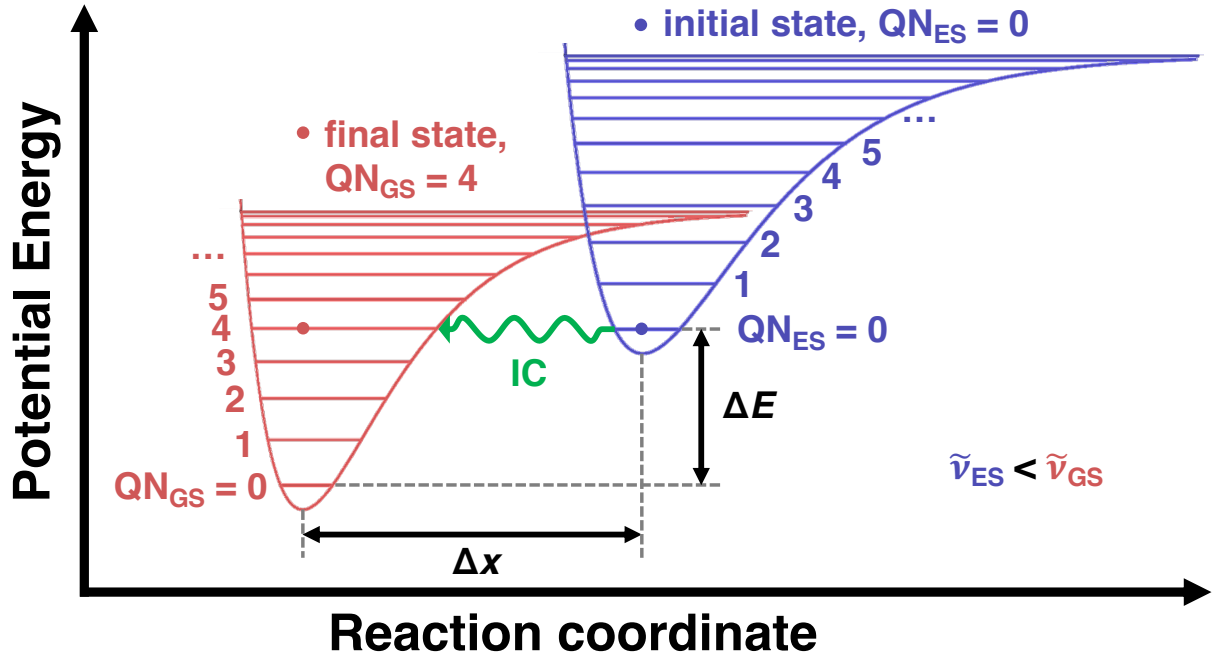

Scheme 2. Potential energy diagram illustrating important factors that control the rate of IC between two vibronic states, namely the initial vibronic state composed of the zeroth vibrational level ($QN_{ES} = 0$, where QN = quantum number) of an electronic excited state (ES) and the final vibronic state composed of the fourth vibrational level ($QN_{GS} = 4$) of the electronic ground state (GS): the structural distortion between energy minima (Δx) and the energy gap between the two electronic states (ΔE). Please note that while the Morse potential energy curves represent potential energies of two states of a diatomic molecule, the vibrational energy levels represented by horizontal lines is total energy or the sum of potential and kinetic energy.

Background

Non-RTs are composed of two fundamental steps: the horizontal (isoenergetic) IC/ISC processes that involve a conversion from one electronic state to another, and vertical vibrational relaxation (VR) processes that dissipate excess energy into the vibrational modes of the solute and solvent (**Scheme 1**). A theoretical description of IC/ISC is often presented within the framework of perturbation theory, where the stationary-state solutions to molecular Hamiltonians are used to derive the rates of transitions caused by a weak perturbation.[57] A more detailed description of theoretical framework is shown in Section S3 of the SI. Here, we describe a more concise outline. The rate $\Gamma_{i\to f}$ for the non-RT from the initial eigenstate i to a density of final eigenstates f that are close in energy to state i can be expressed using Fermi's Golden Rule, as follows:

$$\Gamma_{i\to f} = \frac{2\pi}{\hbar}\left(\int \psi_i \hat{H}_{i\to f} \psi_f d\tau_e\right)^2 \left(\int \chi_i \chi_f d\tau_n\right)^2 \left(\int S_i S_f d\tau_s\right)^2 \qquad (1)$$

This equation is represented in the context of the Born-Oppenheimer approximation and assuming weak spin-orbit coupling. In equation 1, the molecular wavefunctions of the initial and final state,

Ψ_i and Ψ_f, are expressed as a product of fundamental electronic (ψ_i *and* ψ_f), nuclear (χ_i and χ_f) and spin (S_i and S_f) wavefunctions. This equation follows the approach used by Turro et al.[2] The first square term in eq 1 represents the electronic coupling matrix $|V_k|^2$. The integral in the first square term is carried over electronic coordinates τ_e for electronic wavefunctions $\psi(\tau_e; \tau_n)$ with explicit dependence on electronic coordinates τ_e and parametric dependence on the nuclear coordinates τ_n. For non-RTs, this $|V_k|^2$ parameter will be large for nuclear motion that promotes the mixing of the initial and final states. For example, consider an electronic transition that transforms a *p*-like orbital of the carbon atom to a hybrid sp^n orbital (**Scheme 3**). In this case, out-of-plane bending vibrations involving that carbon atom have a strong effect on the electronic coupling matrix values and allow transitions between orbitals of different symmetry.[2] In contrast, the in-plane vibrations will have a small value of $|V_k|^2$ and will not significantly encourage the electronic transition.[2]

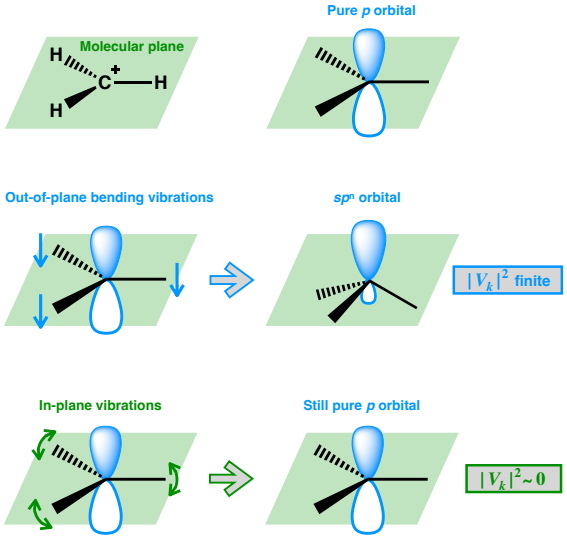

Scheme 3. The effect of different vibrations with varying magnitudes of the electronic coupling matrix $|V_k|^2$ on the *p* orbital of a carbenium ion. Adapted with permission from N. J. Turro, V. Ramamurthy and J. C. Scaiano's *Principles of Molecular Photochemistry*.[2]

The second squared term in eq 1 is called the FCF, a dimensionless parameter that ranges from 0 to 1. In polyatomic molecules with *N* atoms, the molecular vibrational wavefunction is represented as a product of wavefunctions of 3*N*–6 (or 3*N*–5 for linear molecules) vibrational modes. Here, we will assume that a molecule contains only one promoting and one accepting vibrational mode, which is a suitable model for describing a diatomic molecule. Alternatively, the one-dimensional model used here can represent a critical mode of a polyatomic molecule that is effective at causing IC, while all remaining modes are assumed not to participate in IC. In the MATLAB/Python code provided here, the FCF is calculated by squaring the integral of the product of the nuclear wavefunction of the initial zero vibrational level ($QN_{ES} = 0$) of electronic excited state, χ_i, and the nuclear wavefunction of the final vibrationally "hot" level (QN_{GS}) of the electronic ground state, χ_f. Both nuclear wavefunctions are treated as normalized harmonic oscillator wavefunctions. The integration is over the full $[-\infty, +\infty]$ range of nuclear coordinates τ_n, but in practice is carried out over a defined region $[x_{\min}, x_{\max}]$ around the origin, which is where the minimum of the potential

energy well of the ground electronic state is located and where the nuclear wavefunctions have significant amplitudes (eq 2).

$$\mathrm{FCF} = \left[\int_{-\infty}^{+\infty} \chi_i \chi_f dx\right]^2 \approx \left[\int_{-x_{\min}}^{x_{\max}} \psi_{\mathrm{ES},0}(\alpha_{\mathrm{ES}}, x - \Delta x)\psi_{\mathrm{GS,QN}}(\alpha_{\mathrm{GS}}, x)dx\right]^2 \qquad (2)$$

Here, Δx represents the distortion, i.e., a displacement between the potential energy surface minima of the initial and final state (**Scheme 2**). This parameter will be varied by students to derive an intuitive understanding of how it affects rates of IC. The normalized quantum harmonic oscillator wavefunctions, $\psi_{\mathrm{ES},0}(\alpha_{\mathrm{ES}}, x - \Delta x)$ and $\psi_{\mathrm{GS,QN}}(\alpha_{\mathrm{GS}}, x)$ are written using Hermite polynomials,[58] as shown in eq 3a-c:

$$\psi_{\mathrm{QN}}(x) = (2^{\mathrm{QN}}\mathrm{QN}!)^{-1/2}(\alpha/\pi)^{1/4}e^{-\alpha x^2/2}H_{\mathrm{QN}}\left(\alpha^{1/2}x\right) \qquad (3a)$$

where the Hermite polynomials are defined as shown in eq 3b

$$H_{\mathrm{QN}}\left(\alpha^{1/2}x\right) = (-1)^{\mathrm{QN}}e^{\left(\alpha^{1/2}x\right)^2}\frac{d^{\mathrm{QN}}e^{-\left(\alpha^{1/2}x\right)^2}}{d(\alpha^{1/2}x)^{\mathrm{QN}}} \qquad (3b)$$

and the simplifying frequency parameter, α, is defined as

$$\alpha = 2\pi\nu\mu/\hbar \qquad (3c)$$

where ν is the vibrational frequency and μ is the reduced mass.

The value $\mathrm{QN_{GS}}$ is obtained from the energy gap ΔE, as shown in eq 4 and illustrated in **Scheme 2**. Students will be able to change the value of ΔE, to learn how the optical gap affects the rates of non-RTs. Unlike the decreasing Morse potential level spacing approaching the dissociation energy illustrated in **Scheme 2**, energy levels in our simple quantum harmonic oscillator model are evenly spaced:

$$E_{\mathrm{QN}} = \left(\mathrm{QN} + \frac{1}{2}\right)h\nu = \left(\mathrm{QN} + \frac{1}{2}\right)hc\tilde{\nu}, \mathrm{QN} = 0,1,2, \ldots \qquad (4a)$$

where $\tilde{\nu}$ is the user-defined vibrational wavenumber. To determine the quantum number of the final vibrational level in the electronic ground state, $\mathrm{QN_{GS}}$, that is energetically accessible from $\mathrm{QN_{ES}} = 0$ of the electronic excited state, we divide the energy gap ΔE by the quantized energy interval of the ground state $hc\tilde{\nu}_{\mathrm{GS}}$ (or $h\nu_{\mathrm{GS}}$) and round to the nearest integer:

$$\mathrm{QN_{GS}} = \left\lceil\frac{\Delta E}{hc\tilde{\nu}_{\mathrm{GS}}}\right\rfloor \qquad (4b)$$

The rounding to the nearest integer is done using the "round" functions both in MATLAB[59] and in the Python NumPy library.[60]

The third square term in eq 1 introduces the spin and distinguishes between IC and ISC. Although an integral of spin wavefunctions over the spin coordinate τ_s is written in the third square term, the integral is not evaluated by calculus in the same way as the first two integrals of eq 1. This is due to the limited number of discrete spin states and the orthonormality of spin wavefunctions. Formally, when $S_i = S_f$, then $\int S_i S_f d\tau_s = 1$ and the process is considered IC and is spin-allowed, thus occurring at relatively fast rates. When $S_i \neq S_f$, $\int S_i S_f d\tau_s \sim 0$ and the process is formally spin-forbidden and corresponds to ISC. The "forbidden" spin factor results in a rate of ISC that is orders of magnitude slower than IC unless sufficiently strong spin-orbit coupling takes place. In this teaching module, we consider IC processes, where the spin integral is equal to 1. Therefore, eq 1 can be rewritten for the rate of non-RTs, k_{nr}, as

$$k_{\mathrm{nr}} = \Gamma_{i\to f} = \frac{2\pi}{\hbar}(1\ \mathrm{J}^{-1})(hcV_k)^2(\mathrm{FCF})(1)^2 \tag{5}$$

This technology report focuses on how FCFs from eq 4 affect the rate of IC. While V_k will be a parameter entered by the user and can be computed using electronic structure software, for the purpose of the modules presented here, we will keep V_k constant at 750 cm^{-1}, which needs to be converted into energy by $E = hc\tilde{\nu} = hcV_k$ as shown in eq 5. As stated above, we also assume that only a single vibrationally hot electronic ground state contributes to the overall transition probability and leave out the density of states term to avoid summing or integrating over several states that may be energetically accessibility in an ensemble of molecules. The goal is to provide students with an intuition of how structural distortion (Δx), the energy gap (ΔE) and vibrational wavenumbers ($\tilde{\nu}_{\mathrm{ES}}$ and $\tilde{\nu}_{\mathrm{GS}}$) affect the rate of IC, as shown in **Scheme 2**.

Modules

Examples of the outputs from the MATLAB and Python codes that are based on eqs 3-7 for visualizing wavefunction overlap are shown in **Figure S1** and **Figures 1-3**. Three teaching modules are provided, as summarized in **Table S1** in Section S5 of the SI.

Teaching Module 1: FCF versus displacement (Δx). The first module is designed to teach students about the effect of the horizontal geometric displacement (Δx) between the excited state and ground state equilibrium structures on the FCF. For this module, students can change the Δx input parameter to see how the FCF, and thereby k_{nr}, changes with displacement (**Figure 1**), using the "FCF vs Displacement" MATLAB/Python code. For transitions involving higher vibrational levels of the ground electronic state (ground state vibrational quantum number $\mathrm{QN_{GS}} > 0$), students will see that the FCF increases and then decreases as Δx increases (See **Figure 1A**). This is due to increasing wavefunction overlap at values of x farther from equilibrium with increasing vibrational quantum number. The FCF then decreases exponentially at larger Δx as the wavefunction overlap decreases while the wavefunctions move further apart. When Δx is 0 Å, FC overlap will be 0 for any non-zero energy gap, since the harmonic oscillator wavefunctions are orthogonal. Due to the orthonormality of the harmonic oscillator wave functions at Δx = 0 Å, the FCF is 1 when $\mathrm{QN_{GS}}$ = 0 and 0 when the $\mathrm{QN_{GS}} > 0$, which can be emphasized to students.

At small displacements, the FCF increases with displacement for $QN_{GS} > 0$. This means that if a molecule undergoes excited-state distortion, it is less likely to exhibit photoemission due to the competing non-RT that occurs at faster rate due to the large FCF. Such excited-state distortions have been shown in many cases to decrease excited state lifetimes (details in Section S6 of Supporting Information).[61-65]

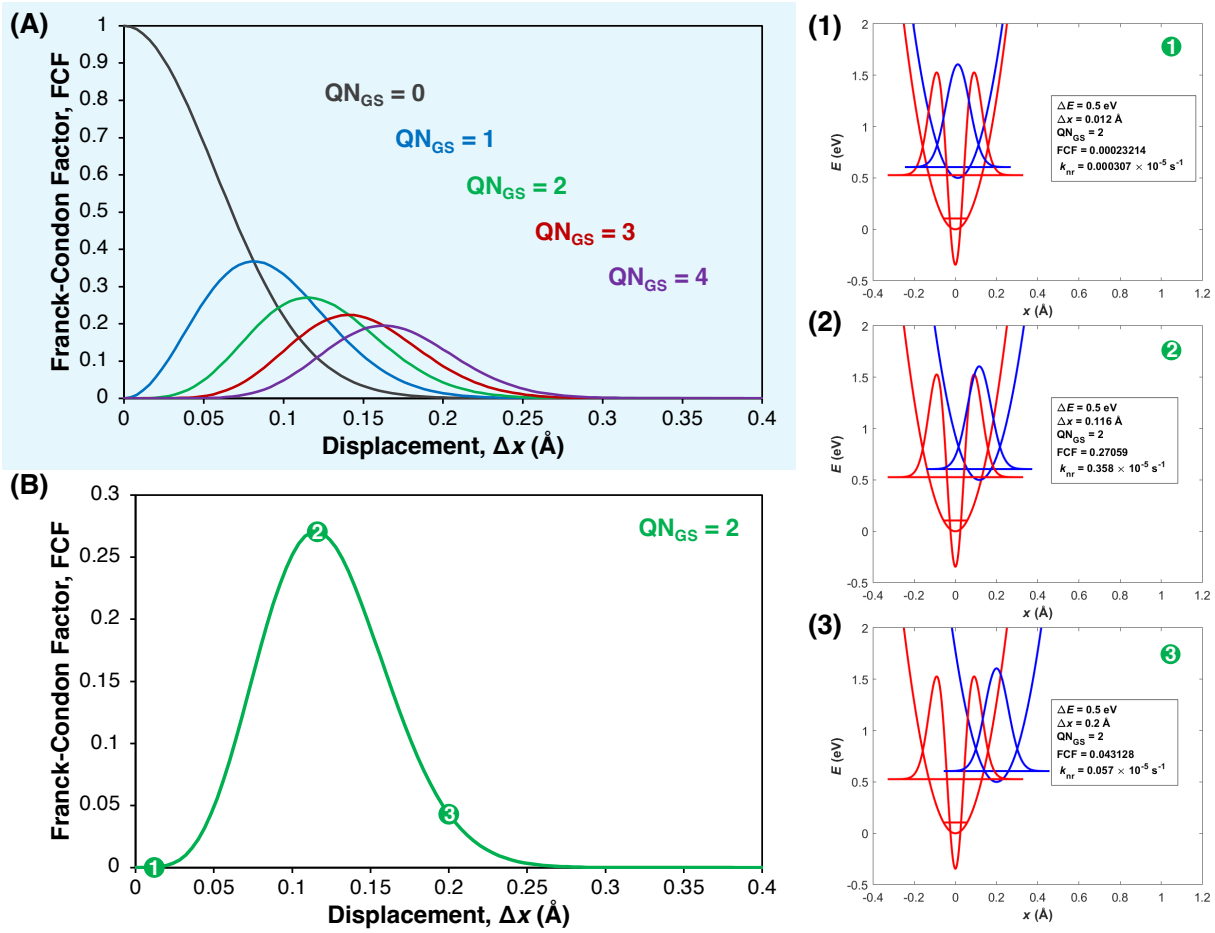

Figure 1. (A) Plots of FCF as a function of Δx for several ground state QN (QN_{GS}) values: 0 (gray), 1 (blue), 2 (green), 3 (red), and 4 (purple). (B) For $QN_{GS} = 2$, the FCF first increases and then decreases as Δx increases. This is demonstrated by the 3 snapshots of the FC overlap for $QN_{GS} = 2$ at Δx = (1) 0.012 Å, (2) 0.116 Å and (3) 0.2 Å.

Teaching Module 2: FCF versus energy gap (ΔE). The second module uses the same MATLAB/Python code as Module 1 to generate the wavefunction overlap plots. For this module, students can change the input for the vertical electronic energy gap (ΔE). The MATLAB code will produce the quantum number for the vibrationally excited electronic ground state wavefunction and illustrate the corresponding harmonic oscillator wavefunction, while the electronic excited state wavefunction remains at the vibrational ground state, represented with the harmonic oscillator function with quantum number 0. The graph will show the quantum number for the ground state wavefunction along with the FCF and k_{nr} values. Students can vary the electronic energy gap to see how it affects the FCF and k_{nr} values (see **Figure 2** and plot a graph like **Figure 2A**) by using

the "FCF vs Energy Gap" MATLAB/Python code. As the energy gap is adjusted by a student, the code will produce the QN for the ground state and FCF values for varying ΔE values.

At displacement smaller than 0.1 Å, we see that the rate of non-RT decreases as the vertical energy gap increases (See **Figure 2A**). This manifests in the EGL, which was first proposed as an empirical relationship by Robinson and Frosch,[66] and then given a more theoretical development by Siebrand,[67] Englman and Jortner,[4] and Fischer.[5] The EGL has been observed in many systems (details in Section S7 of Supporting Information).

While the EGL has been widely reported, it may be violated at larger Δx values, as we see in **Figure 2A**, and even inverted beyond that point, meaning FC overlap increases and then decrease as energy gap increases. While this is rare, this effect has been observed experimentally.[68-73]

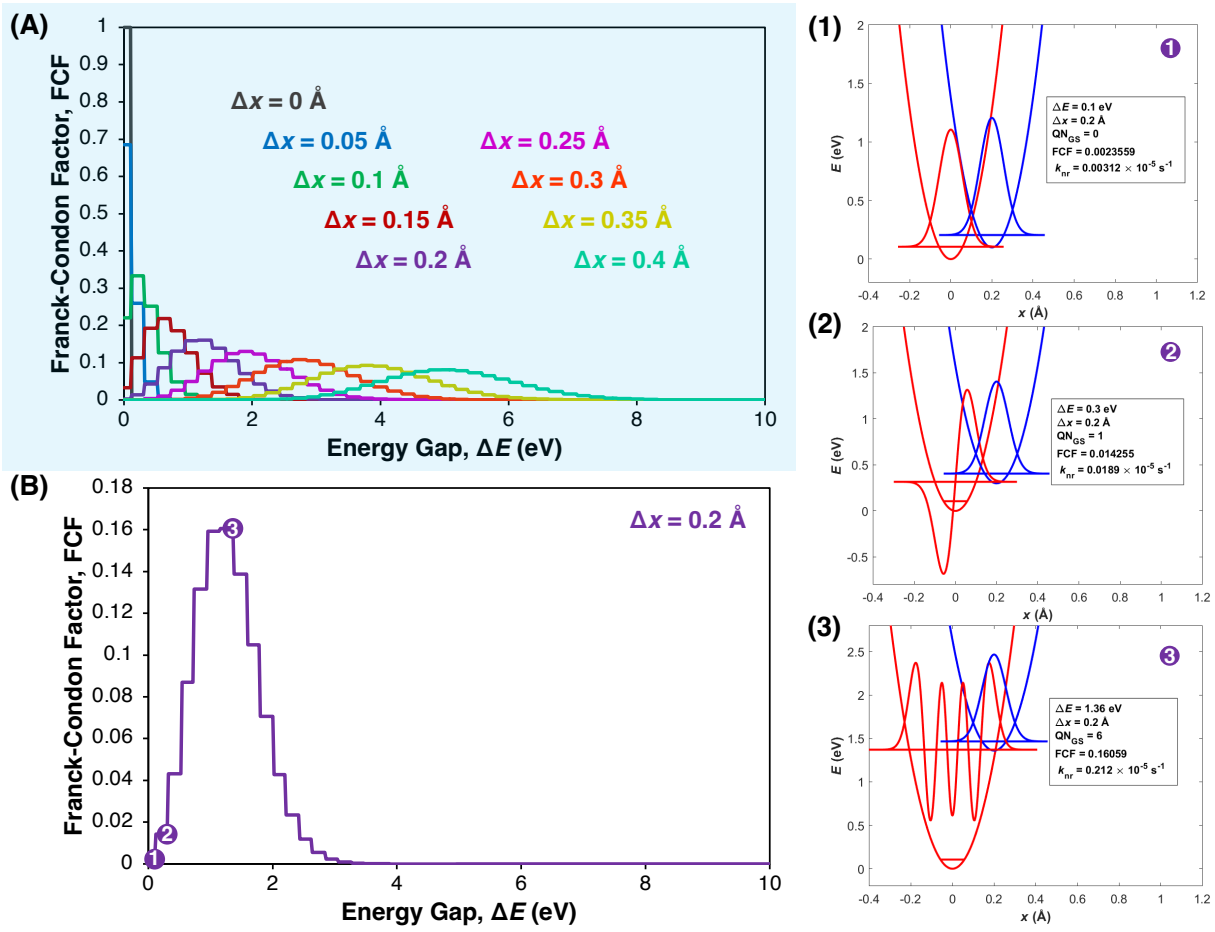

Figure 2. (A) Plots of FCF as a function of ΔE for different Δx values. (B) For Δx = 0.2 Å, the FCF first increases and then decreases as ΔE increases. This is demonstrated by the 3 snapshots of the FC overlap for Δx = 0.2 Å at ΔE = (1) 0.1 eV, (2) 0.3 eV and (3) 1.36 eV.

Teaching Module 3: FCF versus excited state vibrational mode frequencies ($\tilde{\nu}_{ES}$). The third module uses a different MATLAB/Python code for making the wavefunction overlap plots (**Figure S1B**) to show the effect of the frequencies of the vibrational modes of the excited on FCF and k_{nr}. Students can set the displacement and electronic energy gap values to the same numbers and

change the input values for the excited state vibrational mode wavenumber to see how it affects the FC overlap and k_{nr} values (**Figure 3**).

In Modules 1 and 2, students are working with an ideal scenario where the vibrational mode frequencies for the excited and ground states are the same. However, this is rarely the case in practice.[74] By plotting FCF versus excited state vibrational wavenumber for various ground state QN values (**Figure 3A**), it can be seen that the FCF value at $\Delta x = 0$ Å is non-zero only for the even ground state QN values. The excited state wavefunction (QN = 0) has even parity, so without any displacement, multiplying this wavefunction by a wavefunction with odd parity will result in an odd function, which always has an integral of 0. Instructors may use this as an opportunity to discuss the role of parity in overlap integrals with help of this tool that allows students investigate overlaps visually.

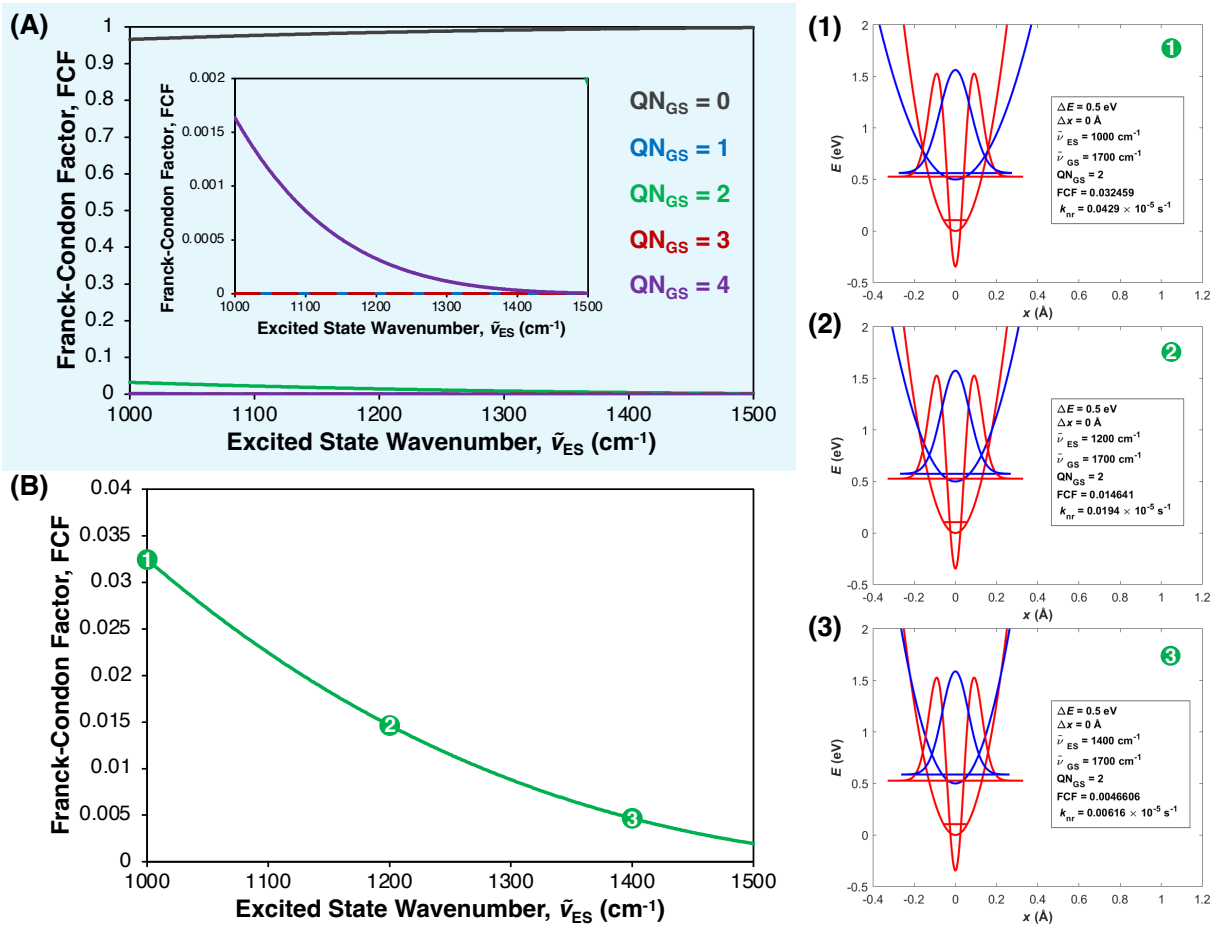

Figure 3. (A) Plots of FCF as a function of excited state vibrational wavenumbers $\tilde{\nu}_{ES}$ when $\tilde{\nu}_{GS}$ = 1700 cm^{-1} for different energy gaps or QN_{GS}. The inset is a zoom-in of the plots of FCF as a function of excited state vibrational wavenumbers for QN_{GS} = 1, 3 and 4. (B) For QN_{GS} = 2, the FCF decreases as $\tilde{\nu}_{ES}$ increases from 1000 cm^{-1} to 1500 cm^{-1}. This is demonstrated by the 3 snapshots of the FC overlap for Δx = 0 Å and ΔE = 0.3 eV at $\tilde{\nu}_{ES}$ = (1) 1000 cm^{-1}, (2) 1200 cm^{-1} and (3) 1400 cm^{-1}.

Classroom Experience

The modules were introduced to 19 graduate students in a 2-hour lecture as part of a physical chemistry seminar course. After providing the theoretical background on non-RTs, students were asked to make hypotheses regarding the effects of various factors that affect the rate of non-RT. Afterwards, students changed the input parameters, e.g., displacement or energy gap from excited state to ground state, in the MATLAB code, visualized the outcome, and discussed whether the results were consistent with their initial hypotheses. Although only a small percentage of the students that were introduced to the activity-based teaching modules had coding experience with MATLAB or Python, all the students completed the tasks requiring changes of input parameters directly in the code by working either individually or in groups. Overall, feedback provided by the students indicated that they found these modules to be an effective and helpful tool to visualize the quantum chemistry concepts associated with molecular spectroscopy. The fact that the students did not need to perform the calculations themselves alleviated the need for the chemistry students to master the mathematics behind the code, making it easier to grasp the underlying principles.

Conclusions

The direct visualization of changes in Franck-Condon overlaps that result from changing excited state displacement from ground state, electronic energy gap between excited state and ground states, and excited state vibrational mode frequencies helps students develop an intuitive understanding of the factors that affect the rate of non-radiative transitions. Furthermore, the understanding of nonradiative decay principles, their ancillary Kasha's rule, the energy gap law, and their exceptions helps students develop a theoretical framework for interpreting experimental electronic spectra and photochemistry.

Associated Content

Supporting Information

The Supporting Information is available at

Expanded Introduction and Background sections, example MATLAB/Python outputs, Teaching Modules summary, application examples of Modules 1 and 2 (PDF)

MATLAB/Python codes and summary slides for each module:

MATLAB file for overlap plot for teaching Modules 1 and 2 (TXT)
MATLAB file for overlap plot for teaching Module 3 (TXT)
MATLAB file for FCF calculation for teaching Module 1 (TXT)
MATLAB file for FCF calculation for teaching Module 2 (TXT)
MATLAB file for FCF calculation for teaching Module 3 (TXT)

Python file for overlap plot for teaching Modules 1 and 2 (TXT)
Python file for overlap plot for teaching Module 3 (TXT)
Python file for FCF calculation for teaching Module 1 (TXT)
Python file for FCF calculation for teaching Module 2 (TXT)

Python file for FCF calculation for teaching Module 3 (TXT)

Slides summarizing MATLAB output for teaching Module 1 (PDF)
Slides summarizing MATLAB output for teaching Module 2 (PDF)
Slides summarizing MATLAB output for teaching Module 3 (PDF)

Author Information

Corresponding Author: Ksenija D. Glusac
Email: glusac@uic.edu

Notes
The authors declare no competing financial interest.

Acknowledgment

We thank the National Science Foundation (award number: 2102247) for support.

References

1. Nelson, T. R.; White, A. J.; Bjorgaard, J. A.; Sifain, A. E.; Zhang, Y.; Nebgen, B.; Fernandez-Alberti, S.; Mozyrsky, D.; Roitberg, A. E.; Tretiak, S., Non-adiabatic Excited-State Molecular Dynamics: Theory and Applications for Modeling Photophysics in Extended Molecular Materials. *Chem Rev* **2020,** *120* (4), 2215-2287.
2. Turro, N. J.; Ramamurthy, V.; Scaiano, J. C., *Principles of molecular photochemistry : an introduction*. University Science Books: Sausalito, Calif., 2009; p xxi, 495 p.
3. Caspar, J. V.; Meyer, T. J., Application of the Energy-Gap Law to Nonradiative, Excited-State Decay. *J Phys Chem-Us* **1983,** *87* (6), 952-957.
4. Englman, R.; Jortner, J., Energy Gap Law for Radiationless Transitions in Large Molecules. *Mol Phys* **1970,** *18* (2), 145-+.
5. Fischer, S., Correlation Function Approach to Radiationless Transitions. *J Chem Phys* **1970,** *53* (8), 3195-3207.
6. Navizet, I.; Liu, Y. J.; Ferré, N.; Roca-Sanjuán, D.; Lindh, R., The Chemistry of Bioluminescence: An Analysis of Chemical Functionalities. *Chemphyschem* **2011,** *12* (17), 3064-3076.
7. Brodl, E.; Winkler, A.; Macheroux, P., Molecular Mechanisms of Bacterial Bioluminescence. *Comput Struct Biotec* **2018,** *16*, 551-564.
8. Miller, S. D.; Haddock, S. H. D.; Elvidge, C. D.; Lee, T. F., Detection of a bioluminescent milky sea from space. *P Natl Acad Sci USA* **2005,** *102* (40), 14181-14184.
9. Giuliani, G.; Melaccio, F.; Gozem, S.; Cappelli, A.; Olivucci, M., QM/MM Investigation of the Spectroscopic Properties of the Fluorophore of Bacterial Luciferase. *J Chem Theory Comput* **2021,** *17* (2), 605-613.
10. Gozem, S.; Mirzakulova, E.; Schapiro, I.; Melaccio, F.; Glusac, K. D.; Olivucci, M., A Conical Intersection Controls the Deactivation of the Bacterial Luciferase Fluorophore. *Angew Chem Int Edit* **2014,** *53* (37), 9870-9875.

11. Salem, L., Surface Crossings and Surface Touchings in Photochemistry. *J Am Chem Soc* **1974,** *96* (11), 3486-3501.
12. Bernardi, F.; Olivucci, M.; Robb, M. A., Potential energy surface crossings in organic photochemistry. *Chemical Society Reviews* **1996,** *25* (5), 321-328.
13. Becker, R. S.; Dolan, E.; Balke, D. E., Vibronic Effects in Photochemistry - Competition between Internal Conversion and Photochemistry. *J Chem Phys* **1969,** *50* (1), 239-245.
14. Kochendoerfer, G. G.; Mathies, R. A., Spontaneous emission study of the femtosecond isomerization dynamics of rhodopsin. *J Phys Chem-Us* **1996,** *100* (34), 14526-14532.
15. Gozem, S.; Luk, H. L.; Schapiro, I.; Olivucci, M., Theory and Simulation of the Ultrafast Double-Bond lsomerization of Biological Chromophores. *Chem Rev* **2017,** *117* (22), 13502-13565.
16. Polli, D.; Altoè, P.; Weingart, O.; Spillane, K. M.; Manzoni, C.; Brida, D.; Tomasello, G.; Orlandi, G.; Kukura, P.; Mathies, R. A.; Garavelli, M.; Cerullo, G., Conical intersection dynamics of the primary photoisomerization event in vision. *Nature* **2010,** *467* (7314), 440-443.
17. Rieke, F.; Baylor, D. A., Single-photon detection by rod cells of the retina. *Rev Mod Phys* **1998,** *70* (3), 1027-1036.
18. McCusker, J. K., Electronic structure in the transition metal block and its implications for light harvesting. *Science* **2019,** *363* (6426), 484-488.
19. Condon, E. U., Nuclear motions associated with electron transitions in diatomic molecules. *Phys Rev* **1928,** *32* (6), 0858-0872.
20. Condon, E., A theory of intensity distribution in band systems. *Phys Rev* **1926,** *28* (6), 1182-1201.
21. Franck, J., Elementary processes of photochemical reactions. *T Faraday Soc* **1926,** *21* (3), 0536-0542.
22. Harris, D. C.; Bertolucci, M. D., *Symmetry and spectroscopy : an introduction to vibrational and electronic spectroscopy*. Dover: New York, 1989; p xii, 550 pages.
23. Levine, I. N., *Molecular spectroscopy*. Wiley: New York, 1975; p x, 491 pages : illustrations.
24. Fong, F. K., *Radiationless Processes : in Molecules and Condensed Phases*. 1st 1976. ed.; Springer Berlin Heidelberg : Imprint: Springer: Berlin, Heidelberg, 1976.
25. Bernath, P. F., Spectra of atoms and molecules. Fourth edition. ed.; Oxford University Press,: New York, 2020; p. 1 online resource.
26. Birks, J. B., *Photophysics of aromatic molecules*. Wiley-Interscience: London, New York,, 1970; p xiii, 704 p.
27. Engel, T.; Reid, P., *Quantum chemistry and spectroscopy*. 3rd ed.; Pearson: Boston, 2013; p xvi, 507 p.
28. Siebrand, W., Radiationless Transitions in Polyatomic Molecules .I. Calculation of Franck-Condon Factors. *J Chem Phys* **1967,** *46* (2), 440-447.
29. Ito, A.; Meyer, T. J., The Golden Rule. Application for fun and profit in electron transfer, energy transfer, and excited-state decay. *Phys Chem Chem Phys* **2012,** *14* (40), 13731-13745.
30. Koç, H., Analytical Evaluation for Calculation of Two-Center Franck-Condon Factor and Matrix Elements. *J Chem-Ny* **2018,** *2018*.
31. Nicholls, R. W., Franck-Condon Factors to High Vibrational Quantum Numbers I - N2 and N+2. *J Res Nat Bur Stand* **1961,** *A 65* (5), 451-460.
32. Luis, J. M.; Bishop, D. M.; Kirtman, B., A different approach for calculating Franck-Condon factors including anharmonicity. *J Chem Phys* **2004,** *120* (2), 813-822.

33. Bicer, O. F.; Lomlu, R.; Katmer, F.; Süzer, S., Franck-Condon Factors in Electronic Excitations from the Ground and Excited Vibrational States Are Different. *J Chem Educ* **2023,** *100* (6), 2423-2429.
34. Chang, J. L., A new formula to calculate Franck-Condon factors for displaced and distorted harmonic oscillators. *J Mol Spectrosc* **2005,** *232* (1), 102-104.
35. Gozem, S.; Krylov, A. I., The ezSpectra suite: An easy-to-use toolkit for spectroscopy modeling. *Wires Comput Mol Sci* **2022,** *12* (2), e1546.
36. Levine, I. N., *Physical chemistry*. 6th ed.; McGraw-Hill: Boston, 2009; p xviii, 989 p.
37. McQuarrie, D. A.; Simon, J. D., *Physical chemistry : a molecular approach*. University Science Books: Sausalito, Calif., 1997; p xxiii, 1270 p.
38. Atkins, P. W.; De Paula, J.; Keeler, J., *Atkins' Physical chemistry*. Eleventh edition. ed.; Oxford University Press: Oxford, United Kingdom ; New York, NY, 2018; p xxvii, 908 pages.
39. Hotta, S., Mathematical Physical Chemistry : Practical and Intuitive Methodology. 1st ed.; Springer Singapore : Imprint: Springer,: Singapore, 2018; pp. 1 online resource (XV, 627 pages 93 illustrations, 32 illustrations in color.
40. Becker, R. S., *Theory and interpretation of fluorescence and phosphorescence*. Wiley Interscience: New York, 1969.
41. Medvedev, E. S.; Osherov, V. I., *Radiationless transitions in polyatomic molecules*. Springer-Verlag: Berlin ; London, 1995; p ix, 374 p : ill.
42. Jaffe, H. H.; Miller, A. L., The fates of electronic excitation energy. *J Chem Educ* **1966,** *43* (9), 469.
43. Rhodes, W., Molecular Excited-State Relaxation Processes. *J Chem Educ* **1979,** *56* (9), 562-567.
44. Camrud, E.; Turner, D. B., A Tractable Numerical Model for Exploring Nonadiabatic Quantum Dynamics. *J Chem Educ* **2017,** *94* (5), 582-591.
45. Fisher, A. A. E., An Introduction to Coding with Matlab: Simulation of X-ray Photoelectron Spectroscopy by Employing Slater's Rules. *J Chem Educ* **2019,** *96* (7), 1502-1505.
46. Marlowe, J.; Tsilomelekis, G., Accessible and Interactive Learning of Spectroscopic Parameterization through Computer-Aided Training. *J Chem Educ* **2020,** *97* (12), 4527-4532.
47. Srnec, M. N.; Upadhyay, S.; Madura, J. D., A Python Program for Solving Schrodinger's Equation in Undergraduate Physical Chemistry. *J Chem Educ* **2017,** *94* (6), 813-815.
48. van Staveren, M., Integrating Python into a Physical Chemistry Lab. *J Chem Educ* **2022**.
49. Goun, A.; Glusac, K. D., Ultrafast Laser Pulse Generation by Mode Locking: MATLAB-Based Demonstrations. *J Chem Educ* **2023,** *100* (2), 955-961.
50. Qiu, J. J.; Moeller, A.; Zhen, J. E.; Yang, H. S.; Din, L.; Adelstein, N., Teaching Heterogeneous Electrocatalytic Water Oxidation with Nickel- and Cobalt-Based Catalysts Using Cyclic Voltammetry and Python Simulation. *J Chem Educ* **2023,** *100* (8), 3036-3043.
51. Stippell, E.; Akimov, A. V.; Prezhdo, O. V., PySyComp: A Symbolic Python Library for the Undergraduate Quantum Chemistry Course. *J Chem Educ* **2023,** *100* (10), 4077-4084.
52. Weiss, C. J., Introduction to Stochastic Simulations for Chemical and Physical Processes: Principles and Applications. *J Chem Educ* **2017,** *94* (12), 1904-1910.
53. Teplukhin, A.; Babikov, D., Visualization of Potential Energy Function Using an Isoenergy Approach and 3D Prototyping. *J Chem Educ* **2015,** *92* (2), 305-309.
54. Konkol, J. A.; Tsilomelekis, G., Porchlight: An Accessible and Interactive Aid in Preprocessing of Spectral Data. *J Chem Educ* **2023,** *100* (3), 1326-1332.

55. Alexander, M. H.; Hall, G. E.; Dagdigian, P. J., The Approach to Equilibrium: Detailed Balance and the Master Equation. *J Chem Educ* **2011,** *88* (11), 1538-1543.
56. Jameson, G.; Brüschweiler, R., Active Learning Approach for an Intuitive Understanding of the Boltzmann Distribution by Basic Computer Simulations. *J Chem Educ* **2020,** *97* (10), 3910-3913.
57. Zhang, J. M.; Liu, Y., Fermi's golden rule: its derivation and breakdown by an ideal model. *Eur J Phys* **2016,** *37* (6), 065406.
58. Levine, I. N.; Jaworski, A., *Quantum chemistry*. Seventh edition. ed.; Pearson: Boston, 2014; p 700 pages.
59. Inc., T. M. *MATLAB version: 9.13.0 (R2022b)*, The MathWorks Inc.: Natick, Massachusetts, United States, 2022.
60. Harris, C. R.; Millman, K. J.; van der Walt, S. J.; Gommers, R.; Virtanen, P.; Cournapeau, D.; Wieser, E.; Taylor, J.; Berg, S.; Smith, N. J.; Kern, R.; Picus, M.; Hoyer, S.; van Kerkwijk, M. H.; Brett, M.; Haldane, A.; del Río, J. F.; Wiebe, M.; Peterson, P.; Gérard-Marchant, P.; Sheppard, K.; Reddy, T.; Weckesser, W.; Abbasi, H.; Gohlke, C.; Oliphant, T. E., Array programming with NumPy. *Nature* **2020,** *585* (7825), 357-362.
61. Lam, E. S. H.; Lam, W. H.; Yam, V. W. W., A Study on the Effect of Dianionic Tridentate Ligands on the Radiative and Nonradiative Processes for Gold(III) Alkynyl Systems by a Computational Approach. *Inorg Chem* **2015,** *54* (7), 3624-3630.
62. Zhu, H.; Fan, J. L.; Li, M.; Cao, J. F.; Wang, J. Y.; Peng, X. J., A "Distorted-BODIPY"-Based Fluorescent Probe for Imaging of Cellular Viscosity in Live Cells. *Chem-Eur J* **2014,** *20* (16), 4691-4696.
63. Yam, V. W. W., Using synthesis to steer excited states and their properties and functions. *Nat Synth* **2023,** *2* (2), 94-100.
64. Li, E. Y.; Cheng, Y. M.; Hsu, C. C.; Chou, P. T.; Lee, G. H., Neutral Ru(II)-based emitting materials: A prototypical study on factors governing radiationless transition in phosphorescent metal complexes. *Inorg Chem* **2006,** *45* (20), 8041-8051.
65. Kreitner, C.; Heinze, K., Excited state decay of cyclometalated polypyridine ruthenium complexes: insight from theory and experiment. *Dalton T* **2016,** *45* (35), 13631-13647.
66. Robinson, G. W.; Frosch, R. P., Electronic Excitation Transfer and Relaxation. *J Chem Phys* **1963,** *38* (5), 1187-1203.
67. Siebrand, W., Radiationless Transitions in Polyatomic Molecules .2. Triplet-Ground-State Transitions in Aromatic Hydrocarbons. *J Chem Phys* **1967,** *47* (7), 2411-2422.
68. Cai, J. J.; Lim, E. C., Naphthalylnaphthalene, a Molecule with Remarkable Photophysical Properties - Violation of the Energy-Gap Law in Radiationless Transitions. *J Chem Phys* **1991,** *95* (4), 3014-3016.
69. Shi, J. Q.; Izquierdo, M. A.; Oh, S.; Park, S. Y.; Milián-Medina, B.; Roca-Sanjuán, D.; Gierschner, J., Inverted energy gap law for the nonradiative decay in fluorescent floppy molecules: larger fluorescence quantum yields for smaller energy gaps. *Org Chem Front* **2019,** *6* (12), 1948-1954.
70. Fidder, H.; Rini, M.; Nibbering, E. T. J., The role of large conformational changes in efficient ultrafast internal conversion: Deviations from the energy gap law. *J Am Chem Soc* **2004,** *126* (12), 3789-3794.
71. Wei, Y. C.; Wang, S. F.; Hu, Y.; Liao, L. S.; Chen, D. G.; Chang, K. H.; Wang, C. W.; Liu, S. H.; Chan, W. H.; Liao, J. L.; Hung, W. Y.; Wang, T. H.; Chen, P. T.; Hsu, H. F.; Chi, Y.;

Chou, P. T., Overcoming the energy gap law in near-infrared OLEDs by exciton-vibration decoupling. *Nat Photonics* **2020,** *14* (9), 570-577.
72. Wang, Y. H.; Ren, J. J.; Shuai, Z. G., Minimizing non-radiative decay in molecular aggregates through control of excitonic coupling. *Nat Commun* **2023,** *14* (1), 5056.
73. Cravcenco, A.; Yu, Y.; Edhborg, F.; Goebel, J. F.; Takacs, Z.; Yang, Y. Z.; Albinsson, B.; Börjesson, K., Exciton Delocalization Counteracts the Energy Gap: A New Pathway toward NIR-Emissive Dyes. *J Am Chem Soc* **2021,** *143* (45), 19232-19239.
74. Li, G. F.; Parimal, K.; Vyas, S.; Hadad, C. M.; Flood, A. H.; Glusac, K. D., Pinpointing the Extent of Electronic Delocalization in the Re(I)-to-Tetrazine Charge-Separated Excited State Using Time-Resolved Infrared Spectroscopy. *J Am Chem Soc* **2009,** *131* (33), 11656-11657.